AGU PUBLICATIONS

Geophysical Research Letters

RESEARCH LETTER
10.1002/2014GL061047

Key Points:
- The Arctic phytoplankton phenology is shifting from a polar to a temperate mode
- Fall blooms coincide with delayed freezeup and increasing role of storms
- Intensity and frequency of fall storms increased over the last decade

Supporting Information:
- Text S1
- Figure S1
- Figure S2
- Figure S3
- Figure S4
- Figure S5
- Figure S6
- Figure S7
- Table S1

Correspondence to:
M. Ardyna,
Mathieu.Ardyna@takuvik.ulaval.ca

Citation:
Ardyna, M., M. Babin, M. Gosselin, E. Devred, L. Rainville, and J.-É. Tremblay (2014), Recent Arctic Ocean sea ice loss triggers novel fall phytoplankton blooms, *Geophys. Res. Lett.*, *41*, doi:10.1002/2014GL061047.

Received 1 JUL 2014
Accepted 14 AUG 2014
Accepted article online 19 AUG 2014

Recent Arctic Ocean sea ice loss triggers novel fall phytoplankton blooms

Mathieu Ardyna[1], Marcel Babin[1], Michel Gosselin[2], Emmanuel Devred[1], Luc Rainville[3], and Jean-Éric Tremblay[1]

[1]Takuvik Joint International Laboratory, Laval University (Canada) - CNRS (France), Département de biologie et Québec-Océan, Université Laval, Quebec, Quebec, Canada, [2]Institut des sciences de la mer de Rimouski, Université du Québec à Rimouski, Rimouski, Quebec, Canada, [3]Applied Physics Laboratory, University of Washington, Seattle, Washington, USA

Abstract Recent receding of the ice pack allows more sunlight to penetrate into the Arctic Ocean, enhancing productivity of a single annual phytoplankton bloom. Increasing river runoff may, however, enhance the yet pronounced upper ocean stratification and prevent any significant wind-driven vertical mixing and upward supply of nutrients, counteracting the additional light available to phytoplankton. Vertical mixing of the upper ocean is the key process that will determine the fate of marine Arctic ecosystems. Here we reveal an unexpected consequence of the Arctic ice loss: regions are now developing a second bloom in the fall, which coincides with delayed freezeup and increased exposure of the sea surface to wind stress. This implies that wind-driven vertical mixing during fall is indeed significant, at least enough to promote further primary production. The Arctic Ocean seems to be experiencing a fundamental shift from a polar to a temperate mode, which is likely to alter the marine ecosystem.

1. Introduction

The Arctic sea ice cover is undergoing an unprecedented decline [*Overland et al.*, 2014; *Serreze et al.*, 2007]. From 1979 to 2012, the September ice extent decreased by an average of 14 ± 3% per decade, accompanied by drastic changes in sea ice thickness [*Overland and Wang*, 2013]. An increasing surface area of the Arctic Ocean is thus exposed to direct sunlight during summer and fall, resulting in a longer season for phytoplankton growth [*Arrigo et al.*, 2008]. Analyses of satellite-sensed ocean color data suggest that, as a consequence, the Pan-Arctic annual phytoplankton primary production has increased by more than 20% since 1998 [*Arrigo and van Dijken*, 2011; *Bélanger et al.*, 2013]. Other observations, however, show an enhanced upper ocean stratification driven by increases in river discharge of buoyant freshwater to the Arctic Ocean, as for instance, in the Beaufort Gyre [*Morison et al.*, 2012; *Yamamoto-Kawai et al.*, 2009]. This process reduces vertical mixing and thus decreases the input of nutrients from the deep pool to the sunlit surface layer. The phytoplankton community has responded to this change in stratification by increasing the abundance of small-sized species typical of oligotrophic regimes [*Li et al.*, 2009]. Differences in vertical mixing and upward nutrient resupply during fall/winter (i.e., before freezeup) are likely responsible for the observed variability in the productivity of spring blooms across the Arctic Ocean [*Tremblay and Gagnon*, 2009], whereas the inorganic nutrients provided by rivers have little impact beyond local estuarine transition zones [*Le Fouest et al.*, 2013].

Decline in the summer extent of the ice pack allows increased air-ocean exchange of momentum, moisture, and heat, which enhances the strength and size of Arctic storms [*Long and Perrie*, 2012; *Simmonds and Keay*, 2009]. Such storms promote vertical mixing and nutrient replenishment to the well-lit surface layer [*Pickart et al.*, 2013; *Zhang et al.*, 2013]. A key and vigorously debated question about possible changes in primary production and marine ecosystems in the Arctic Ocean is whether the decrease in summer sea ice, which increases light availability and lengthens the growing season, is also conducive to enhanced vertical mixing and thereby only to additional primary production.

The phenology of phytoplankton blooms can be observed using time series of surface chlorophyll *a* concentrations derived from ocean-color remote sensing [*Chiswell et al.*, 2013; *Sapiano et al.*, 2012; *Vargas et al.*, 2009; *Zhai et al.*, 2012]. At temperate latitudes, two phytoplankton blooms develop every year: a main one in spring when light availability is high, the mixed layer is shallow and nutrients are abundant due to winter deep mixing; and a secondary bloom during late summer/early fall (denoted here as "fall") when light

availability is still relatively high and storm-driven mixing replenishes nutrients in the upper well-lit layer. At high latitudes, the spring bloom occurs without a subsequent fall bloom. The absence of a fall bloom can be attributed to a combination of several processes: (1) light is limited by low Sun elevation and/or sea ice formation, (2) strong stratification, and/or (3) sea ice freezeup inhibits wind-driven vertical mixing and nutrient replenishment of the well-lit surface layer. Here we present an unexpected consequence of Arctic ice loss: regions that experienced a single annual bloom only a decade ago now develop a second bloom in the fall.

2. Materials and Methods

2.1. Satellite Data and Time Series Analysis

Satellite-derived chlorophyll *a* (chl *a*) concentrations from Sea-viewing Wide Field-of-view Sensor (SeaWiFS) (1998–2002) and Moderate Resolution Imaging Spectroradiometer (MODIS) (2003–2012) daily Level 3 were downloaded from NASA's ocean color website (http://oceandata.sci.gsfc.nasa.gov) for latitude greater than 50°N. The standard OC4v4 and OC3 algorithms for SeaWiFS and MODIS, respectively [*O'Reilly et al.*, 1998], were used to retrieve chl *a* concentration. A new 25 km resolution grid was generated, and rather than averaging the 9 km (SeaWiFS) and 4 km (MODIS) pixels within a 25 km grid cell, the value of each SeaWiFS and MODIS pixel was kept to avoid any loss of information during fitting. For example, for a given day, if five MODIS pixels were available in a 25 km grid cell, these data were not averaged, but stored and used in the locally weighted scatterplot smoothing (LOESS) (see section 2.2 and the supporting information for details). Daily satellite-derived sea ice concentration data from Special Sensor Microwave Imager (SSMI) (1998–2007) and SSMI/Sounder (2008–2012) sensors were obtained from the National Snow and Ice Data Center (NSIDC, http://nsidc.org) [*Cavalieri et al.*, 1996; *Maslanik and Stroeve*, 1999]. Values of each SeaWiFS and MODIS pixel in area where sea ice concentration was greater than 10% were discarded to avoid possible contamination of the ocean color signal [*Arrigo and van Dijken*, 2011; *Bélanger et al.*, 2007, 2013]. To compensate for the scarce number of valid pixels in the Arctic Ocean due to sea ice and cloud cover, the daily chl *a* data were aggregated over three time periods (i.e., without any averaging for time series analysis) according to the following years: 1998–2001, 2002–2006, and 2007–2012. This partitioning was chosen based on changes in September sea ice extent during 1998–2012 using a test for significant differences (analysis of variance test, $p < 0.001$, see the supporting information and Figure S4 for details).

To infer the number of stormy days, we used the reanalysis 2 derived wind data at 10 m with a 6 h temporal resolution from the National Center for Environmental Prediction (NCEP) [*Kalnay et al.*, 1996] (http://www.esrl.noaa.gov/psd). At any given grid point in the data set, the number of stormy days was defined as the total time in days for which the wind speed estimates were higher than 10 m s^{-1} between 1 September and 30 October, which corresponds to a number ranging between 0 and 61 days. The number of stormy days over open waters was obtained by adding the condition that the satellite-derived sea ice concentration interpolated to the time and location of the wind estimate is less than 10%. A spatial map of trends was generated using the slopes of the linear regression of the number of stormy days against time in year between 1998 and 2012. Note that only trends (i.e., regression slopes) significantly different from zero ($p < 0.05$) were displayed (within one standard deviation).

2.2. Model of Phytoplankton Phenology

A strategy of forward selection was used to determine the type of phytoplankton annual cycle (see the supporting information for details), which means that incremental complexity (i.e., addition of new terms) of the model was tested for significance (i.e., $p < 0.05$) [*Sapiano et al.*, 2012; *Vargas et al.*, 2009]. In other words, if the addition of a new term was not proved statistically significant, the previous model was chosen to be the most representative of the phytoplankton annual cycle. The optimization of the parameters and the evaluation of the statistical significance of added terms in our step-by-step approach were performed using a nonlinear least squares optimization function (*nls*(); package *stats* in *R*). The simplest model was a straight line of slope 0 and intercept β_0 which corresponds to a constant value of chl *a* concentration. The most complex parameterization of the phytoplankton annual cycle was a two-peak Gaussian model superimposed over a background concentration of phytoplankton [*Zhai et al.*, 2012], which is expressed as follows:

$$\mathrm{chl}\,a\,(t) = \beta_0 + a_1 e^{\left(-\frac{(t-t_{m1})^2}{2\sigma_1^2}\right)} + a_2 e^{\left(-\frac{(t-t_{m2})^2}{2\sigma_2^2}\right)}, \quad (1)$$

where subscripts 1 and 2 refer to the first and second peak of phytoplankton biomass, β_0 is the background chl *a* concentration (mg chl *a* m^{-3}), a_i corresponds to the amplitude of peak $i = 1, 2$ (mg chl *a* m^{-3}), $t_{m,i}$

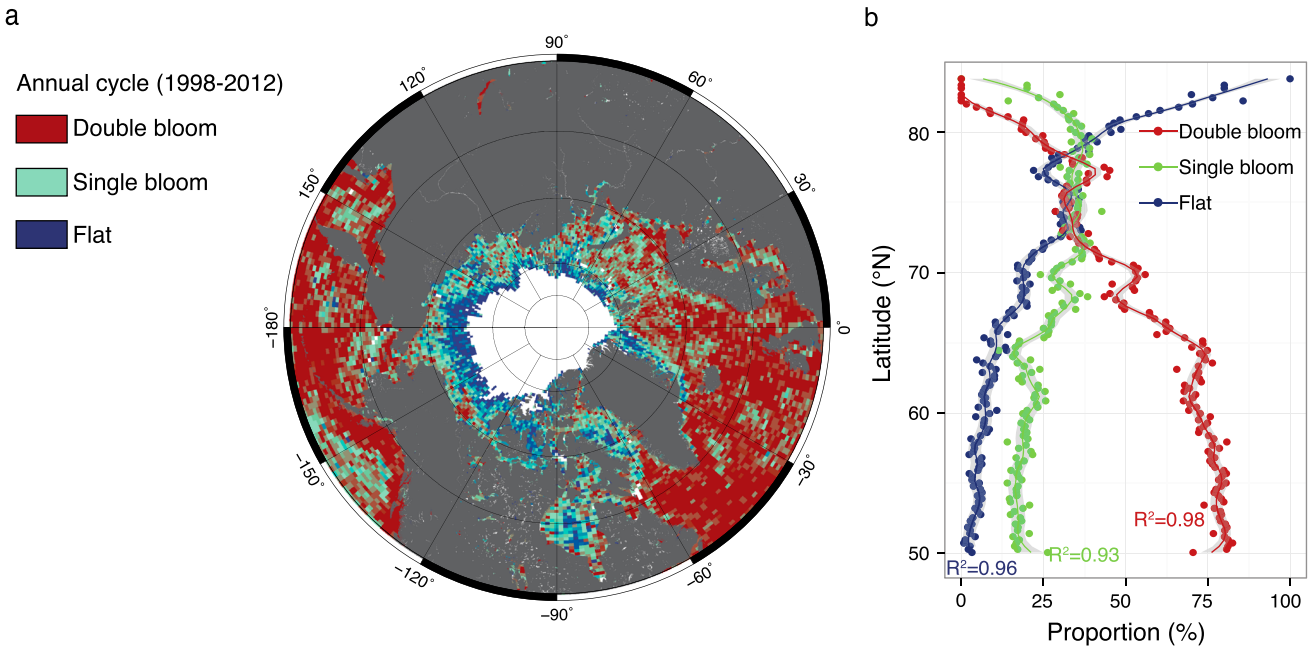

Figure 1. Phytoplankton phenology above 50°N. (a) Climatology (1998–2012) of the different types of annual cycles (i.e., flat, single bloom, or double bloom). The white area corresponds to the minimum sea ice cover over the period 1998–2012 and the void of remotely sensed ocean color data. (b) Latitudinal proportion of each phenology. The smoothing of each phenology is obtained using a LOESS polynomial fit (span = 0.13). Shaded areas provide confidence intervals (0.95 significance level).

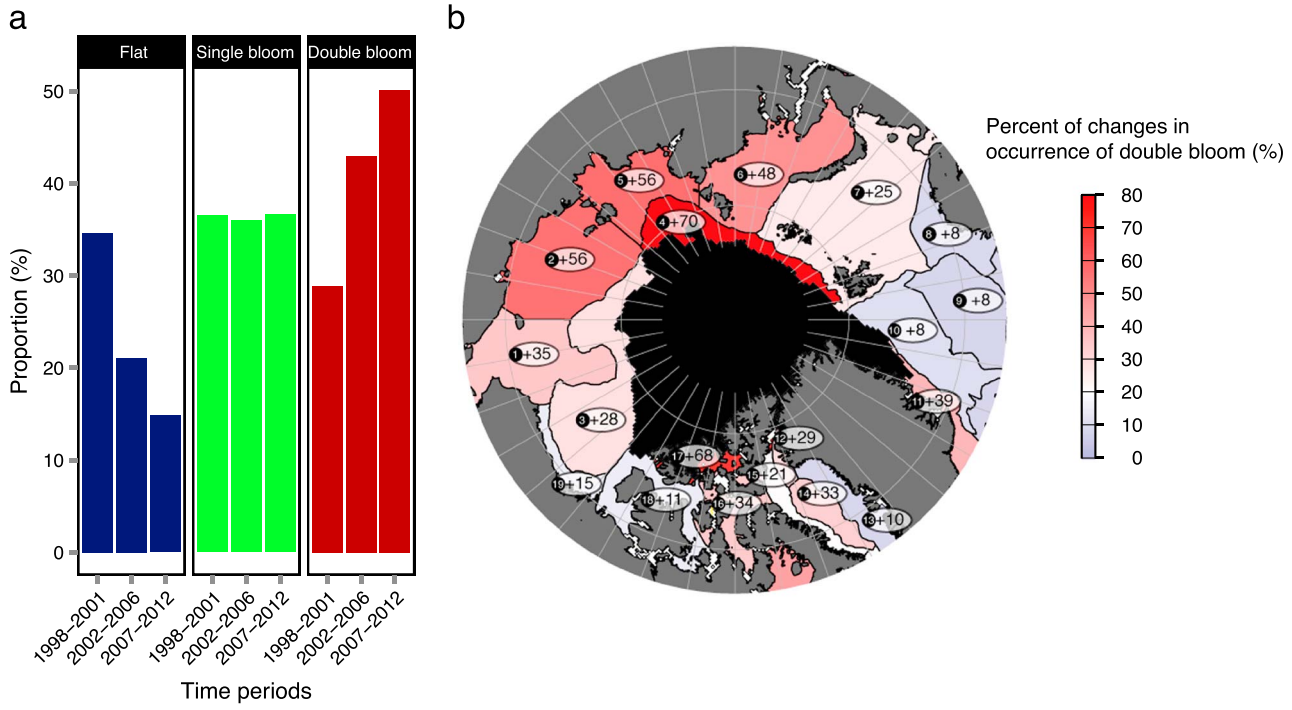

Figure 2. Current shifts in Arctic phytoplankton phenology above the Arctic Circle (>66.58°N). (a) Histogram of different types of annual cycles for three periods (1998–2001, 2002–2006, and 2007–2012). (b) Map adapted from the World Wildlife Fund agency showing percent change in double bloom occurrence between two periods (1998–2001 versus 2007–2012) for each Arctic region (numbered within dark circles): (1) Chukchi Sea, (2) East Siberian Sea, (3) central Arctic Ocean – Canadian Basin, (4) central Arctic Ocean – Eurasian Basin, (5) Laptev Sea, (6) Kara Sea, (7) North and East Barents Sea, (8) northern Norway and Finnmark, (9) Norwegian Sea, (10) Fram Strait – Greenland Sea, (11) East Greenland Shelf, (12) North Greenland, (13) West Greenland Shelf, (14) Baffin Bay, (15) Baffin Bay – Canadian Shelf, (16) Lancaster Sound, (17) Arctic Archipelago, (18) Beaufort – Amundsen – Viscount Melville – Queen Maud, and (19) Beaufort Sea – continental coast and shelf. The minimum September sea ice extent in 2012 is indicated in dark color.

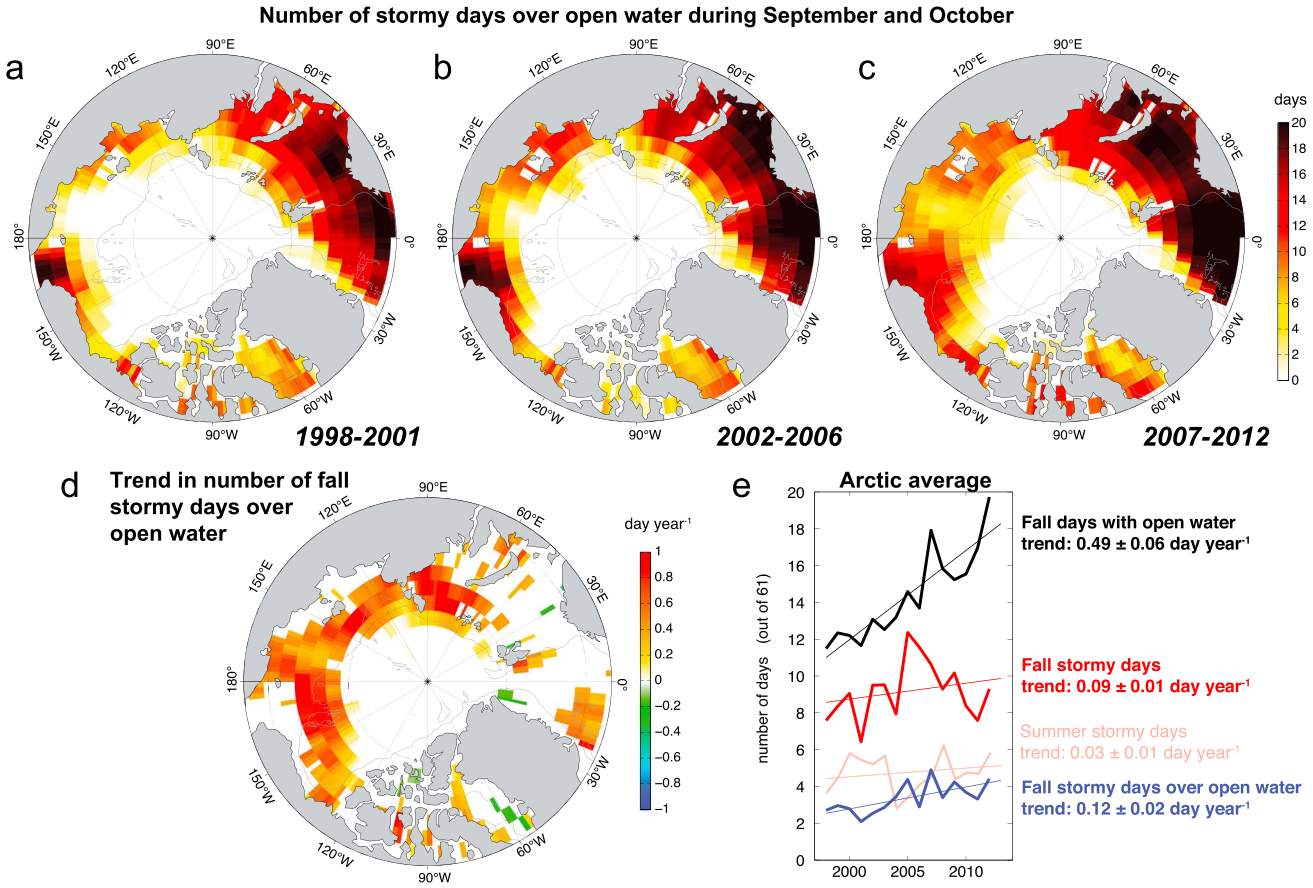

Figure 3. Interplay between wind forcing and open water during fall in the Arctic Ocean. (a–c) Maps of the number of days in September and October when wind speed is higher than 10 m s^{-1} and ice concentrations are smaller than 10%, per year, averaged for three different periods. (d) Trends in the number of stormy days over open water between 1998 and 2012. (e) Time series of the Arctic-wide average of ice-free days (black), stormy days (red), and stormy days over open water (blue) in September and October of each year. Number of stormy days during the summer (July–August, pink) is plotted for reference. Arctic-wide trends are listed with a 95% confidence interval.

is the time when peaks $i = 1, 2$ reaches the maximum (day), and σ_i represents the width (day) at half the maximum of peak $i = 1, 2$.

Using 15 years (1998–2012) of remotely sensed ocean color data, we established annual time series of chl *a* concentration at the ocean surface for each pixel of the 25 km resolution Arctic grid and produced a climatological (time-averaged) spatial map of the three dominant annual phytoplankton cycles: flat, single bloom, or double bloom (Figure 1).

3. Results and Discussion

At temperate latitudes, a double bloom (both spring and fall) dominates in the northern Atlantic and Pacific oceans (~75% of occurrences, see Figure 1b). Moving north from Greenland, the Bering and Labrador seas (above 65°N), the single annual phytoplankton bloom pattern increases at the expense of the double bloom pattern. These single blooms dominate the Arctic seas at latitudes above 73°N, especially in the Western Arctic Ocean. However, in the eastern Arctic Ocean influenced by Atlantic waters (i.e., Norwegian and Greenland seas), both spring and fall blooms remain the main feature of phytoplankton phenology. Above 80°N, a ring of flat annual cycles (no discernible bloom) is associated with the ice edge along the annual minimum ice extent.

When comparing three periods (1998–2001, 2002–2006, and 2007–2012), and selecting only the areas that were seasonally sea ice free above the Arctic Circle (>66.58°N) for all three periods, we found a shift from the flat pattern of ice edges to one and two annual phytoplankton blooms over the last 15 years

(χ^2 test, $p < 0.001$, Figure 2a). Fall blooms have become more common in most regions of the Arctic Ocean (Figure 2b). This phenological shift may be amplified in the future if the growing season continues to lengthen across the Arctic Ocean (see the supporting information, Figures S7a–S7c).

To test whether these changes in phytoplankton bloom phenology were related to changes in wind-driven mixing in the moderately stratified waters of the high Arctic, we calculated the number of high-wind events over regions of open waters. A conservative minimum wind speed threshold of 10 m s^{-1} was selected to induce vertical mixing in sea ice free arctic waters as documented in previous studies [*Long and Perrie*, 2012; *Pickart et al.*, 2013; *Rainville and Woodgate*, 2009; *Simmonds and Keay*, 2009]. Our results show that the average number of stormy days over open waters during September and October significantly increased during the last decade over most of the Arctic Ocean (Figures 3a–3d). This trend results from the combined increase in surface area of open waters and the increase in the frequency and intensity of fall storms (Figure 3e), as suggested by model simulations [*Long and Perrie*, 2012]. Concurrently, the sea ice cover reaches its minimum in September [*Overland and Wang*, 2013], a period where the number of stormy days doubles over the last decade (Figure 3e).

Observations and models show that storms over ice-free waters input momentum in the ocean, driving near-inertial motions in the surface mixed layer, instabilities, and vertical mixing [*Alford and Gregg*, 2001; *Jochum et al.*, 2013]. Wind-driven mixing and the incidental upward supply of nutrients trigger fall blooms at temperate latitudes [*Chiswell et al.*, 2013] and could well be the cause of incipient fall blooms at high latitudes, provided that wind stress is sufficient to weaken the strong vertical stratification. This scenario is consistent with observations collected with moored sensors in the southern Chukchi Sea showing significant increase in near-inertial current speeds in the water column and large vertical current shear, and presumably vertical mixing, extending late into the fall, until the area is covered by newly formed ice [*Rainville and Woodgate*, 2009]. Interestingly, the fall bloom appears to be damped in regions where the accumulation of freshwater is largest and vertical stratification is strongest [*Morison et al.*, 2012] (see also the western Canada Basin in Figure 2b). Thus, changes in phytoplankton phenology appear to be regional and increasing light availability will have an impact on annual primary production and the development of new fall blooms in regions where wind-driven mixing can penetrate deep enough to bring nutrients to the surface [*Ardyna et al.*, 2011]. On the other hand, the impact of light availability will be small or negligible in regions of the Arctic Ocean where strong stratification inhibits wind-driven mixing.

The alteration of marine Arctic ecosystems clearly goes beyond the early onset of phytoplankton blooms [*Kahru et al.*, 2010]; the "polar" paradigm of a single bloom and subsequent sedimentation of organic matter is being challenged at high northern latitudes. In addition to recent northward migrations of temperate species in Arctic waters [*Grebmeier et al.*, 2006], a phenology of biological productivity with two phytoplankton blooms and two peaks of sedimentation may become prevalent. The copepods *Calanus hyperboreus* and *Calanus glacialis*, currently the dominant phytoplankton grazers on Arctic shelves, have been shown to be able to exploit episodic fall phytoplankton blooms, by increasing their recruitment and, presumably, that of carnivores higher up in the food web [*Forest et al.*, 2011; *Tremblay et al.*, 2011]. In a changing Arctic Ocean, the spring bloom will undoubtedly remain the major annual primary production event for carbon export to higher trophic levels and sequestration [*Ardyna et al.*, 2013; *Wassmann et al.*, 1991]. However, changes in phytoplankton phenology or additional pulses of phytoplankton primary production may alter the food web structure and lead to major ecosystem level changes in an environment where consumers must make the most of the short productive period before the long winter sets in. The observations reported in this study undoubtedly challenge the current understanding of Arctic ecosystems and provides new insights into their future.

Acknowledgments

SeaWiFS and MODIS data were made available by the NASA's ocean color group at http://oceandata.sci.gsfc.nasa.gov. Sea ice concentration and NCEP Reanalysis data were, respectively, provided by the NSIDC from their website http://nsidc.org and by the NOAA/OAR/ESRL PSD, Boulder, Colorado, USA, at http://www.esrl.noaa.gov/psd/. We gratefully acknowledge P. Franks, M.-H. Forget, A. Baya, and the whole Takuvik team for constructive comments on initial versions of the manuscript, and two anonymous reviewers for constructive and insightful reviews. We also thank M. Benoît-Gagné for programming assistance, and C. Brown and D. Christiansen-Stowe for language support. M.A. received a postgraduate scholarship from the Canada Excellence Research Chair (CERC) in Remote Sensing of Canada's New Arctic Frontier and stipends from ArcticNet and Québec-Océan. This is a contribution to the research programs of the CERC in Remote Sensing of Canada's New Arctic Frontier, Takuvik Joint International Laboratory, ArcticNet, ISMER, and Québec-Océan.

The Editor thanks two anonymous reviewers for their assistance in evaluating this paper.

References

Alford, M. H., and M. C. Gregg (2001), Near-inertial mixing: Modulation of shear, strain and microstructure at low latitude, *J. Geophys. Res.*, *106*(C8), 16,947–16,968, doi:10.1029/2000JC000370.

Ardyna, M., M. Gosselin, C. Michel, M. Poulin, and J. É. Tremblay (2011), Environmental forcing of phytoplankton community structure and function in the Canadian High Arctic: Contrasting oligotrophic and eutrophic regions, *Mar. Ecol. Prog. Ser.*, *442*, 37–57.

Ardyna, M., M. Babin, M. Gosselin, E. Devred, S. Bélanger, A. Matsuoka, and J. É. Tremblay (2013), Parameterization of vertical chlorophyll *a* in the Arctic Ocean: Impact of the subsurface chlorophyll maximum on regional, seasonal, and annual primary production estimates, *Biogeosciences*, *10*(6), 4383–4404.

Arrigo, K. R., and G. L. van Dijken (2011), Secular trends in Arctic Ocean net primary production, *J. Geophys. Res.*, *116*, C09011, doi:10.1029/2011JC007151.

Arrigo, K. R., G. van Dijken, and S. Pabi (2008), Impact of a shrinking Arctic ice cover on marine primary production, *Geophys. Res. Lett.*, *35*, L19603, doi:10.1029/2008GL035028.
Bélanger, S., J. K. Ehn, and M. Babin (2007), Impact of sea ice on the retrieval of water-leaving reflectance, chlorophyll *a* concentration and inherent optical properties from satellite ocean color data, *Remote Sens. Environ.*, *111*(1), 51–68.
Bélanger, S., M. Babin, and J. É. Tremblay (2013), Increasing cloudiness in Arctic damps the increase in phytoplankton primary production due to sea ice receding, *Biogeosciences*, *10*(6), 4087–4101.
Cavalieri, D. J., C. Parkinson, P. Gloersen, and H. J. Zwally (1996), Sea ice concentrations from Nimbus-7 SMMR and DMSP SSM/I passive microwave data, [1998-2007].
Chiswell, S. M., J. Bradford-Grieve, M. G. Hadfield, and S. C. Kennan (2013), Climatology of surface chlorophyll *a*, autumn-winter and spring blooms in the southwest Pacific Ocean, *J. Geophys. Res. Oceans*, *118*, 1003–1018, doi:10.1002/jgrc.20088.
Forest, A., V. Galindo, G. Darnis, S. Pineault, C. Lalande, J.-É. Tremblay, and L. Fortier (2011), Carbon biomass, elemental ratios (C:N) and stable isotopic composition ($\delta^{13}C$, $\delta^{15}N$) of dominant calanoid copepods during the winter-to-summer transition in the Amundsen Gulf (Arctic Ocean), *J. Plankton Res.*, *33*(3), 161–178.
Grebmeier, J. M., J. E. Overland, S. E. Moore, E. V. Farley, E. C. Carmack, L. W. Cooper, K. E. Frey, J. H. Helle, F. A. McLaughlin, and S. L. McNutt (2006), A major ecosystem shift in the northern Bering Sea, *Science*, *311*(5766), 1461–1464.
Jochum, M., B. P. Briegleb, G. Danabasoglu, W. G. Large, N. J. Norton, S. R. Jayne, M. H. Alford, and F. O. Bryan (2013), The impact of oceanic near-inertial waves on climate, *J. Climate*, *26*(9), 2833–2844.
Kahru, M., V. Brotas, M. Manzano-Sarabio, and B. G. Mitchell (2010), Are phytoplankton blooms occurring earlier in the Arctic?, *Global Change Biol.*, *17*(4), 1733–1739.
Kalnay, E., et al. (1996), The NCEP/NCAR 40-year reanalysis project, *Bull. Am. Meteorol. Soc.*, *77*(3), 437–471.
Le Fouest, V., M. Babin, and J. É. Tremblay (2013), The fate of riverine nutrients on Arctic shelves, *Biogeosciences*, *10*(6), 3661–3677.
Li, W. K. W., F. A. McLaughlin, C. Lovejoy, and E. C. Carmack (2009), Smallest algae thrive as the Arctic Ocean freshens, *Science*, *326*(5952), 539.
Long, Z., and W. Perrie (2012), Air-sea interactions during an Arctic storm, *J. Geophys. Res.*, *117*, D15103, doi:10.1029/2011JD016985.
Maslanik, J. A., and J. C. Stroeve (1999), Near-real-time DMSP SSM/I-SSMIS daily polar gridded sea ice concentrations, [2008-2012].
Morison, J., R. Kwok, C. Peralta-Ferriz, M. Alkire, I. Rigor, R. Andersen, and M. Steele (2012), Changing Arctic Ocean freshwater pathways, *Nature*, *481*(7379), 66–70.
O'Reilly, J. E., S. Maritorena, B. G. Mitchell, D. A. Siegel, K. L. Carder, S. A. Garver, M. Kahru, and C. McClain (1998), Ocean color chlorophyll algorithms for SeaWiFS, *J. Geophys. Res.*, *103*(C11), 24,937–24,953, doi:10.1029/98JC02160.
Overland, J. E., and M. Wang (2013), When will the summer Arctic be nearly sea ice free?, *Geophys. Res. Lett.*, *40*, 2097–2101, doi:10.1002/grl.50316.
Overland, J. E., M. Wang, J. E. Walsh, and J. C. Stroeve (2014), Future Arctic climate changes: Adaptation and mitigation time scales, *Earth's Future*, *2*(2), 68–74.
Pickart, R. S., M. A. Spall, and J. T. Mathis (2013), Dynamics of upwelling in the Alaskan Beaufort Sea and associated shelf–basin fluxes, *Deep Sea Res., Part 1*, *76*(0), 35–51.
Rainville, L., and R. A. Woodgate (2009), Observations of internal wave generation in the seasonally ice-free Arctic, *Geophys. Res. Lett.*, *36*, L23604, doi:10.1029/2009GL041291.
Sapiano, M. R. P., C. W. Brown, S. Schollaert Uz, and M. Vargas (2012), Establishing a global climatology of marine phytoplankton phenological characteristics, *J. Geophys. Res.*, *117*, C08026, doi:10.1029/2012JC007958.
Serreze, M. C., M. M. Holland, and J. Stroeve (2007), Perspectives on the Arctic's shrinking sea-ice cover, *Science*, *315*(5818), 1533–1536.
Simmonds, I., and K. Keay (2009), Extraordinary September Arctic sea ice reductions and their relationships with storm behavior over 1979–2008, *Geophys. Res. Lett.*, *36*, L19715, doi:10.1029/2009GL039810.
Tremblay, J. É., and J. Gagnon (2009), The effects of irradiance and nutrient supply on the productivity of Arctic waters: A perspective on climate change, in *Influence of Climate Change on the Changing Arctic and Sub-Arctic Conditions*, edited by J. C. J. Nihoul and A. G. Kostianoy, pp. 73–93, Springer, Dordrecht, Netherlands.
Tremblay, J. É., et al. (2011), Climate forcing multiplies biological productivity in the coastal Arctic Ocean, *Geophys. Res. Lett.*, *38*, L18604, doi:10.1029/2011GL048825.
Vargas, M., C. W. Brown, and M. R. P. Sapiano (2009), Phenology of marine phytoplankton from satellite ocean color measurements, *Geophys. Res. Lett.*, *36*, L01608, doi:10.1029/2008GL036006.
Wassmann, P., R. Peinert, and V. Smetacek (1991), Patterns of production and sedimentation in the boreal and polar Northeast Atlantic, *Polar Res.*, *10*(1), 209–228.
Yamamoto-Kawai, M., F. A. McLaughlin, E. C. Carmack, S. Nishino, K. Shimada, and N. Kurita (2009), Surface freshening of the Canada Basin, 2003–2007: River runoff versus sea ice meltwater, *J. Geophys. Res.*, *114*, C00A05, doi:10.1029/2008JC005000.
Zhai, L., et al. (2012), Phytoplankton phenology and production around Iceland and Faroes, *Cont. Shelf Res.*, *37*(0), 15–25.
Zhang, J., R. Lindsay, A. Schweiger, and M. Steele (2013), The impact of an intense summer cyclone on 2012 Arctic sea ice retreat, *Geophys. Res. Lett.*, *40*, 720–726, doi:10.1002/grl.50190.